Photometric redshifts for galaxies in the Spitzer Extragalactic Representative Volume Survey (SERVS)

J. Pforr*,**, M. Vaccari, M. D. Lacy, C. Maraston, L. Marchetti
*janine.pforr@esa.int, RF **Pforr et al. 2017

SERVS in a nutshell

(PI: M. Lacy, www.its.caltech.edu/~mlacy/servs.html)

- Spitzer Space Telescope warm phase survey at 3.6 and 4.5 microns
- Imaging of ~18 square degrees in centres of 5 extragalactic fields: SWIRE XMM-LSS, ELAIS-S1, ELAIS-N1, CDFS, Lockman Hole
- ~ 4 million detected sources!
- Overlaps: VISTA-VIDEO near-IR, Herschel-HERMES, SCUBA2-S2CLS far-IR

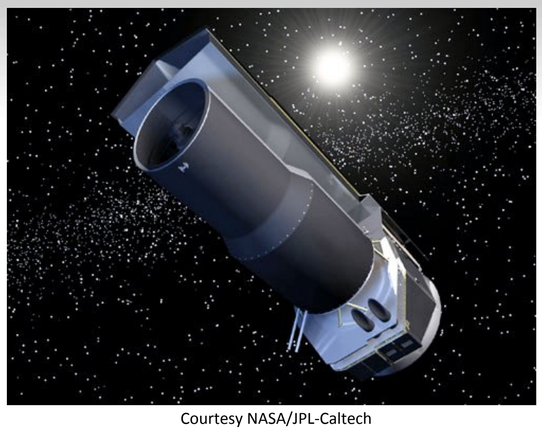

Courtesy NASA/JPL-Caltech

Photometric redshifts - method

Spectral Energy Distribution (SED) Fitting: χ^2 minimization of difference between galaxy template SED fluxes and observed, optical/near-IR/IR fluxes for each object from SERVS Data Fusion (Vaccari 2016a,b) using HyperZ (Bolzonella+ 2000) and Maraston (2005) templates.

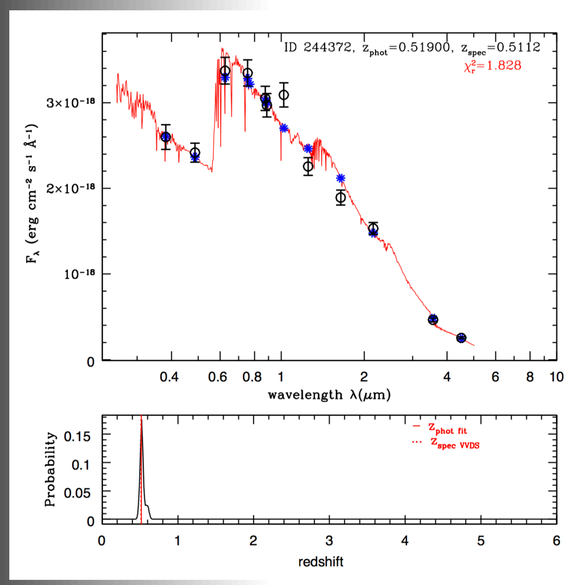

Fig. 1 (left): Top: Example best fit SED template fit (red curve) for object ID 244372 in the XMM field. Blue asterisks: predicted fluxes from the template fit in the given filter bands. Black open circles with error bars: observed flux points in the given filter bands. Listed are χ^2_r of the fit, photometric redshift, spectroscopic redshift from the VVDS survey. Bottom: PDF(z) for this object. Dotted vertical line: location of the spectroscopic redshift. Solid vertical line: location of derived photometric redshift.

Photometric redshifts - results

SERVS field	number of filters	number of objects	mean±1σ	*median*	rms	σ_{NMAD}	η
CDFS	⩾ 2	21543	-0.041 ± 0.349	0.008	0.351	0.068	0.180
	> 10, χ^2_r< 3	628	0.013 ± 0.071	0.013	0.072	0.042	0.041
EN1	⩾ 2	1752	-0.069 ± 0.282	-0.018	0.290	0.043	0.099
	> 8, χ^2_r< 3	600	-0.025 ± 0.130	-0.011	0.132	0.038	0.032
ES1	⩾ 2	6986	-0.046 ± 0.270	-0.010	0.274	0.053	0.104
	> 10, χ^2_r< 3	2586	-0.017 ± 0.079	-0.009	0.081	0.042	0.044
LH	⩾ 2	3236	-0.124 ± 0.414	-0.028	0.432	0.065	0.183
	> 8, χ^2_r< 3	103	-0.033 ± 0.137	-0.011	0.141	0.029	0.039
XMM	⩾ 2	42349	-0.037 ± 0.271	-0.004	0.273	0.049	0.091
	> 10, χ^2_r< 3	18953	-0.012 ± 0.099	-0.004	0.100	0.036	0.029

Table 1 (left): photo-z statistics.

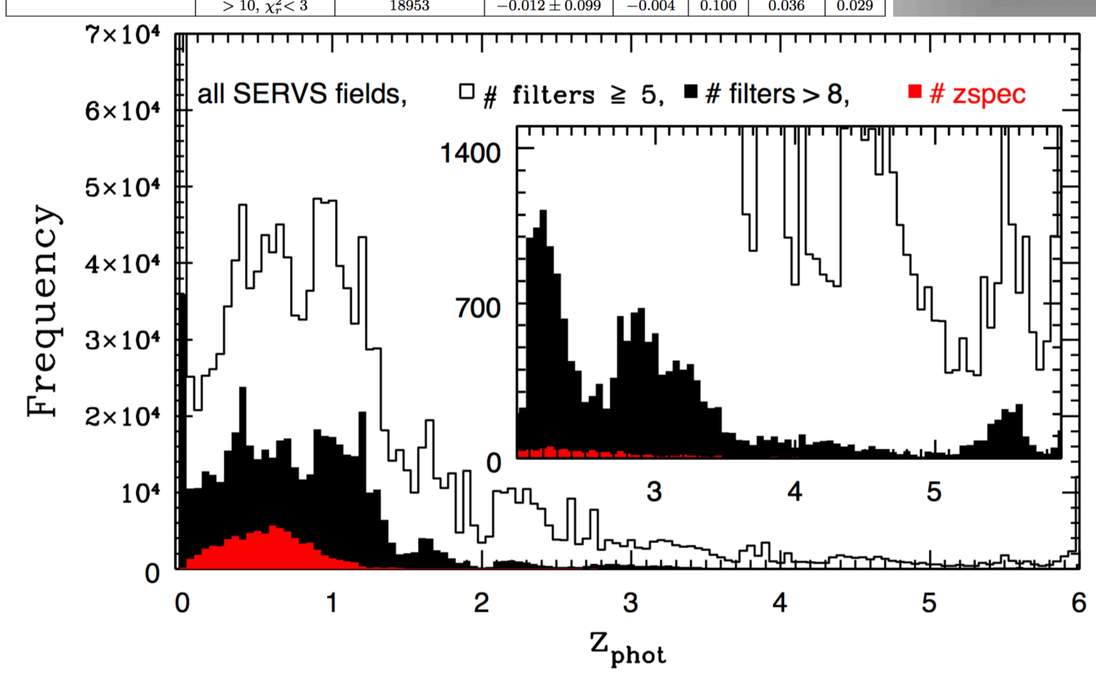

Fig. 4 (top): Photometric redshift distribution for all SERVS fields combined, considering only sources with more than 8 filter bands (shaded histogram) and for all sources with more than 5 filter bands available for the SED-fitting (empty histogram). The distribution of sources with spectroscopic redshift in SERVS is shown via the red shaded histogram.

SERVS Science Goals

Stellar mass assembly

SERVS + VIDEO: photometric redshifts, robust stellar mass estimates for large numbers of high redshift galaxies

Obscured star formation

SERVS + Herschel HERMES, SCUBA2: study obscured star formation at high redshift

The role of AGN

SERVS + SWIRE, Herschel: find normal and obscured quasars

The role of environment

spans wide range of cosmic environments (voids, clusters); investigate how environment of a galaxy affects its star formation history and other properties

The highest redshift quasars

SERVS + VIDEO: detect less luminous z>6 quasars; constrain faint end of the quasar luminosity function at high redshift

Photometric redshifts - testing

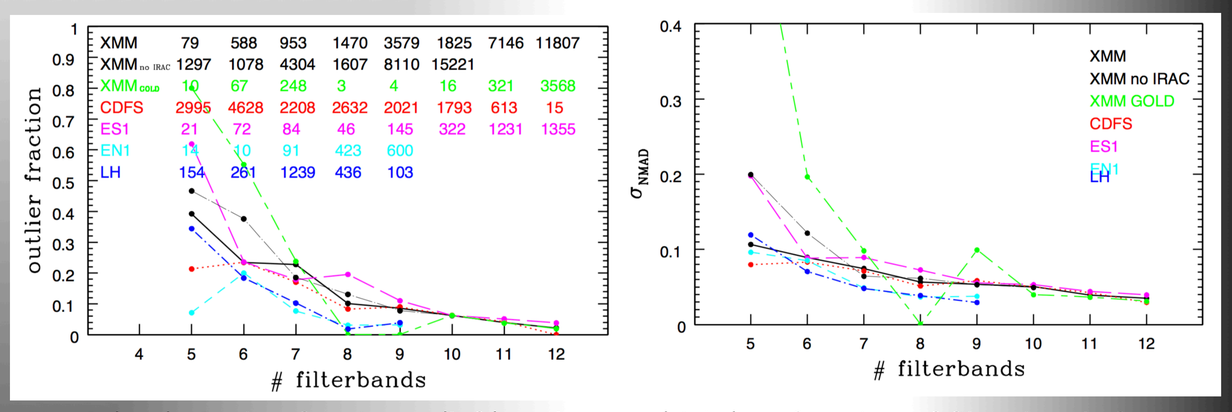

Fig. 2 (top): Outlier fraction η (left) and σ_{NMAD} (right) as function of filter bands for each SERVS field. EN1 = cyan dashed line, LH = blue dashed-dotted line, XMM = solid black line, CDFS = red dotted line, ES1 = long dashed magenta line, XMM without the two SERVS IRAC bands = thin black long-dashed, dotted line, XMM GOLD (subset of full XMM but with tighter matching radius to ancillary data) = green long-dashed, short-dashed line. The total numbers of objects with the according number of filter bands available for the fit are listed as reference. See also Table 1.

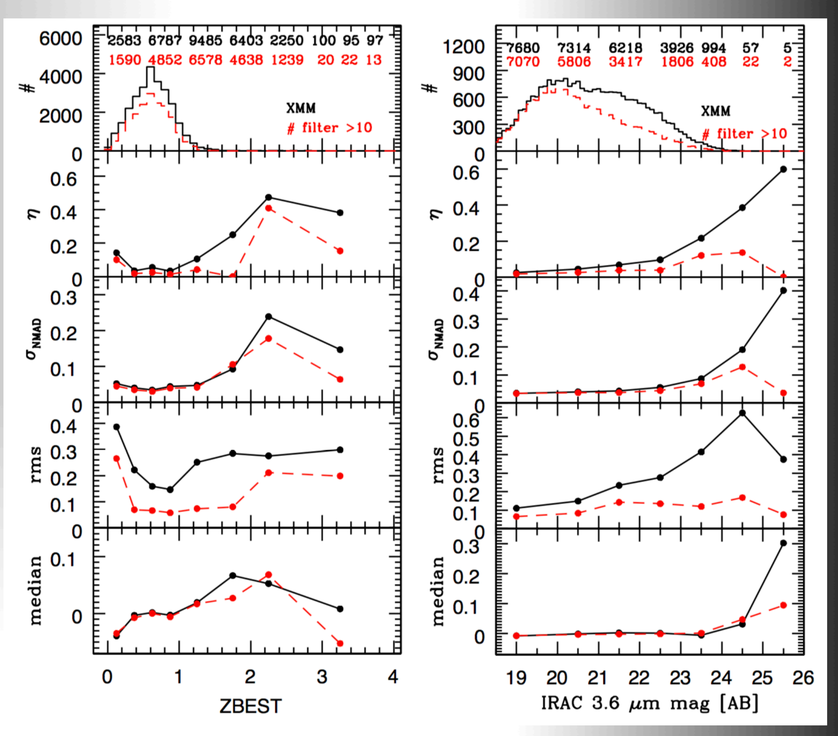

Fig. 3 (left): From top to bottom: Distribution in bins of 0.1, *outlier fraction* η, σ_{NMAD}, *rms* and *median* of $\Delta z / (1+z_{spec})$ as a function of IRAC 3.6 micron AB magnitude (left) for objects with 18 < IRAC 3.6 micron ≤ 26 mag and χ^2_r<3, and spectroscopic redshift ZBEST (right) for objects with 0< z ≤ 4 and χ^2_r<3, for which a spectroscopic redshift is available. η, σ_{NMAD}, *rms* and *median* are derived in bins of 1 mag between 20 mags and 26 mags, and in bins of 2 mags for the brightest magnitudes (18 to 20 mags; left), and in bins of 0.25 between 0<z≤1, in bins of 0.5 between 1<z≤2.5, and for the highest redshift bin from 2.5<z≤4 (right). Points are plotted at the bin centre. The number of objects in each bin is listed in the top panel: black = all objects in that magnitude/redshift and χ^2_r range; red = objects with more than 10 filters in the fitting.

Results and Conclusions

- More filter bands over a large wavelength range result in more robust photometric redshifts.
- For the best photometric setup we achieve σ_{NMAD} ~ 0.035 and an *outlier fraction* η ~3.5 %.
- The exclusion of IRAC bands results in a median small underestimation of photometric redshifts.
- Applying a tighter matching radius of 0.7'' compared to 1'' improves σ_{NMAD} and *outlier fraction* η due to fewer spurious matches.
- In general, σ_{NMAD}, η, *rms* and *median* difference increase with fainter IRAC 3.6 micron AB magnitude due to missing detections in bluer bands of shallower surveys and larger photometric errors at fainter magnitudes. For sources with large numbers of available filter bands this trend is not observed.
- Generally, σ_{NMAD} and η are lowest at z<~1 and increase towards z~2 because higher redshift sources are generally expected to be fainter and lack photometric detections in bluer bands.
- At z<0.5 photometric redshifts are slightly overestimated (*median*), at z>1 photometric redshifts are slightly underestimated.
- We find the majority of SERVS sources below z<1.5. 1.6 % of objects with at least 8 filter bands in the fitting lie at z>3.

Overall, despite the inhomogeneity of the input catalogues, our photometric redshifts are reliable (using >5 filter bands over a wide wavelength range in the SED-fitting), demonstrating that even without more difficult reprocessing of photometry photometric redshifts useful for science analyses can be obtained.

References: Bolzonella M., Miralles J.-M., Pelló R., 2000, A&A, 363, 476 * Maraston C., 2005, MNRAS, 362, 799 * Vaccari M., 2016a, The Universe of Digital Sky Surveys, 42, 71 * Vaccari M., 2016b, ArXiv e-prints